Cancer Chemotherapy and Pharmacology (2019) 83:659–671
https://doi.org/10.1007/s00280-019-03768-8

ORIGINAL ARTICLE

Molecular targeting of HER2-overexpressing biliary tract cancer cells with trastuzumab emtansine, an antibody–cytotoxic drug conjugate

Yoriko Yamashita-Kashima[1] · Yasushi Yoshimura[1] · Takaaki Fujimura[1] · Sei Shu[1] · Mieko Yanagisawa[1] · Keigo Yorozu[1] · Koh Furugaki[1] · Ryota Higuchi[2] · Junichi Shoda[3] · Naoki Harada[1]

Received: 24 July 2018 / Accepted: 5 January 2019 / Published online: 18 January 2019

Abstract

Purpose Trastuzumab emtansine (T-DM1) provides clinical benefit in breast cancers overexpressing human epidermal growth factor receptor 2 (HER2). However, its efficacy against biliary tract cancers (BTC) has not been evaluated. In this study, the effectiveness of T-DM1 in various BTC cell lines and xenograft models with different levels of HER2 expression was investigated.

Methods HER2 expression status in xenografts and patient tissue microarrays was assessed by immunohistochemistry (IHC) or fluorescence in situ hybridization (FISH). Cell-surface HER2 expression levels and cell growth inhibition in response to T-DM1 were examined in 17 BTC cell lines. The antitumor activity of T-DM1 was evaluated in four xenograft mouse models with different levels of HER2 expression. The effects of T-DM1 on HER2 signaling, antibody-dependent cell-mediated cytotoxicity (ADCC), cell cycle, and apoptosis were assessed in vitro.

Results Cell-surface expression of HER2 was observed in both gallbladder carcinoma and cholangiocarcinoma tissues. The anti-proliferative activity of T-DM1 was higher in BTC cell lines and breast cancer cell lines with higher levels of HER2 expression. The HER2 status (IHC score|HER2-to-CEP17 ratio by FISH testing) of each BTC xenograft was 3 +|8.3 for KMCH-1, 2 +|4.7 for Mz-ChA-1, 1 +/0|1.4 for OCUG-1, and 0|1.1 for KKU-100, and T-DM1 showed antitumor activity in proportion to the HER2 status. T-DM1 inhibited HER2 signaling and induced ADCC, mitotic arrest, and apoptosis in KMCH-1 cells.

Conclusions T-DM1 exhibited preclinical activity in HER2-overexpressing BTC. Further evaluation in clinical studies is warranted.

Keywords T-DM1 · Trastuzumab emtansine · HER2 · Biliary tract cancer

Introduction

Biliary tract cancer (BTC) is classified into cholangiocarcinoma (intrahepatic cholangiocarcinoma and extrahepatic cholangiocarcinoma), gallbladder carcinoma, and ampullary carcinoma. BTC is an aggressive solid tumor that is often diagnosed at an advanced disease stage and has a poor outcome with radiation and systemic chemotherapy, such as with gemcitabine and cisplatin [1, 2]. Clinical trials of molecularly targeted therapies, such as erlotinib, lapatinib, cetuximab, sorafenib, and bevacizumab, have been investigated for the treatment of BTC, but their efficacies have not been satisfactory [3]. Thus, a novel therapeutic approach is warranted.

Amplification of human epidermal growth factor receptor (HER) 2 is an oncogenic driver alteration. Protein dimers of

The work was presented, in part, in abstract form at the American Society of Clinical Oncology Gastrointestinal Cancers Symposium; January 18–20, 2018; San Francisco, California, USA.

Yoriko Yamashita-Kashima and Yasushi Yoshimura contributed equally to this work.

Electronic supplementary material The online version of this article (https://doi.org/10.1007/s00280-019-03768-8) contains supplementary material, which is available to authorized users.

✉ Naoki Harada
haradanok@chugai-pharm.co.jp

Extended author information available on the last page of the article

HER2 with HER family receptors, such as epidermal growth factor receptor (EGFR), HER2, HER3, or HER4, accelerate cell proliferation and prolong cell survival [4, 5]. In breast cancer and gastric cancer, HER2 overexpression as a result of gene amplification is a crucial target of HER2-directed agents, including lapatinib, trastuzumab, pertuzumab, and trastuzumab emtansine (T-DM1) [6–8].

HER2 overexpression is also observed in 4.8% (95% CI 0–14.5%) of intrahepatic cholangiocarcinoma, 17.4% (95% CI 3.4–31.4%) of extrahepatic cholangiocarcinoma, 19.1% (95% CI 11.2–26.8%) of gallbladder carcinoma, and 27.9% (95% CI 0-60.7%) of ampullary carcinoma [9], which indicates that overexpression of HER2 could be a promising therapeutic target for BTC; however, so far there is no approved HER2-targeted therapy for patients with BTC. Recently, Nam et al. reported that trastuzumab inhibited cell proliferation in HER2-overexpressing BTC cell lines in vitro by inhibiting the downstream signaling pathways of HER2 that involve RAS/ERK and PI3K/AKT, but the response of HER2-positive BTC patients to trastuzumab combined with chemotherapy was limited [10]. Thus, it is necessary to investigate the potential of HER2-targeted agents other than trastuzumab on HER2-overexpressing BTC.

We previously reported the potency of pertuzumab in combination with trastuzumab in HER2-overexpressing BTC cell lines [11], suggesting that other HER2-targeting agents could be efficacious. T-DM1 is an antibody–drug conjugate composed of trastuzumab covalently linked to DM1, an antimicrotubule agent derived from maytansine. After binding to HER2, T-DM1 is internalized into the cytoplasm and degraded in lysosomes, and the released DM1-containing catabolite binds to tubulin and inhibits the polymerization of tubulins into microtubules [12–14]. In addition, T-DM1 has been reported to retain all of the mechanisms of action of trastuzumab, including antibody-dependent cell-mediated cytotoxicity (ADCC) and inhibition of the PI3K/Akt pathway, which is mediated by trastuzumab binding to HER2 and inhibiting the phosphorylation of HER3 [15]. However, the efficacy of T-DM1 on BTC cells has not yet been demonstrated either in clinical or in preclinical studies. In the present study, we examined the effects of T-DM1 on HER2-overexpressing BTC using HER2-positive and -negative BTC cell lines.

Materials and methods

Test agents

T-DM1 and trastuzumab were provided by F. Hoffmann-La Roche (Basel, Switzerland) as a fine powder and were dissolved in saline and distilled water, respectively. DM1 was purchased from Toronto Research Chemicals (Toronto, Canada) and was dissolved in dimethyl sulfoxide (DMSO). Gemcitabine was purchased from Eli Lilly Japan (Kobe, Japan). Human immunoglobulin G (HuIgG) was purchased from MP Biomedicals (Solon, OH, USA) and was reconstituted with distilled water. T-DM1 was diluted with saline for the in vivo experiments. Each agent was diluted with culture medium for the in vitro experiments.

Animals

Five-week-old male or female BALB/c-nu/nu mice (CAnN.Cg-Foxn1<nu>/CrlCrlj nu/nu) were purchased from Charles River Laboratories Japan (Yokohama, Japan). All animals were acclimatized at least 5 days prior to the study. The health of the mice was monitored daily. The animals were given free access to chlorinated water and irradiated food, and were maintained under a controlled light–dark cycle (12–12 h). All animal experiments were conducted in accordance with the institutional Animal Care and Use Committee at Chugai Pharmaceuticals, Co., Ltd.

Cell lines and culture conditions

The human BTC cell lines used in this study comprised six cholangiocarcinoma cell lines (KKU-055, KKU-100, KKU-213, KMBC, KMCH-1, and SK-ChA-1), seven gallbladder carcinoma cell lines (Mz-ChA-1, Mz-ChA-2, OCUG-1, TGBC-2-TKB, TGBC-14-TKB, TGBC-24-TKB, and TGBC-44-TKB), and four ampullary carcinoma cell lines (TGBC-18-TKB, TGBC-50-TKB, TGBC-51-TKB, and TGBC-52-TKB). KKU-055, KKU-213, and OCUG-1 were obtained from the Japanese Collection of Research Bioresources Cell Bank (Ibaraki, Japan) and TGBC-2-TKB, TGBC-14-TKB, TGBC-18-TKB, TGBC-24-TKB, TGBC-44-TKB, TGBC-50-TKB, TGBC-51-TKB, and TGBC-52-TKB were from the RIKEN BioResource Center Cell Bank (Tsukuba, Japan). KKU-100 was obtained from Dr. B. Sripa (Khon Kaen University, Khon Kaen, Thailand); KMBC and KMCH-1 were from Dr. M. Kojiro (Kurume University School of Medicine, Kurume, Japan); and SK-ChA-1, Mz-ChA-1, and Mz-ChA-2 were from Dr. A. Knuth (Johannes Gutenberg University Mainz, Mainz, Germany). KMCH-1 was maintained in Dulbecco's modified Eagle's medium (DMEM) (Sigma-Aldrich, St. Louis, MO, USA) supplemented with 1 mM sodium pyruvate and 10% heat-inactivated fetal bovine serum (FBS) at 37 °C under 5% CO_2. KMBC was maintained in DMEM supplemented with 20% FBS at 37 °C under 5% CO_2. TGBC-2-TKB was maintained in DMEM supplemented with 5% FBS at 37 °C under 5% CO_2. All other cell lines were maintained in DMEM supplemented with 10% FBS at 37 °C under 5% CO_2.

OCUG-1 was also maintained in BALB/c-nu/nu mice by subcutaneous inoculation of pieces of tumor tissue

for use in the in vivo experiments. As breast cancer cell lines, we used 12 cell lines. BT-483, HCC1806, MCF7, MDA-MB-231, MDA-MB-361, MDA-MB-453, SK-BR-3, T-47D, and ZR-75-1 were obtained from American Type Culture Collection (Manassas, VA, USA); BT-549 was obtained from National Cancer Institute (Frederick, MD, USA); and JIMT-1 was from Deutsche Sammlung von Mikroorganismen und Zellkulturen (Braunschweig, Germany). These cell lines were maintained in conditions recommended by the sources. KPL-4 was obtained from Dr. Kurebayashi (Kawasaki Medical School, Kurashiki, Japan) and maintained as previously described [16]. CD16(158V)/NK-92 (used as the effector cell for ADCC) was constructed and maintained as previously described [17].

Tissue microarrays

Gallbladder carcinoma and cholangiocarcinoma tissue microarrays were obtained from US Biomax (Derwood, MD, USA) and Provitro (Berlin, Germany), respectively.

In vitro cell growth inhibition assay

Cells were seeded onto 96-well plates and pre-cultured for 1 day. Then the cells were treated with T-DM1, DM1, or gemcitabine for 4 days. The cell growth inhibitory activity of T-DM1 and DM1 was examined by quantifying the DNA with Hoechst 33258 nucleic acid stain using a FluoReporter Blue Fluorometric dsDNA Quantitation Kit (Thermo Fisher Scientific, Waltham, MA, USA). Cells were also examined after pre-culturing for 1 day (pre-cultured wells). Fluorescence intensity was measured using excitation at 355 nm and emission at 460 nm with a POLARstar Omega microplate reader (BMG Labtech, Ortenberg, Germany). The percentage of cell growth was calculated as (fluorescence intensity of treated well-fluorescence intensity of pre-cultured well)/(fluorescence intensity of non-treated well-fluorescence intensity of pre-cultured well) × 100.

In vivo tumor growth inhibition study

Mice were inoculated subcutaneously in the right flank with either 5×10^6 cells/mouse of BTC cell line KKU-100, KMCH-1, or Mz-ChA-1, or an approximately 8 mm^3 piece of OCUG-1 tumor tissue. Mice were also inoculated in the right second mammary gland with 5×10^6 cells/mouse of the breast cancer cell line KPL-4. Several weeks after inoculation, mice were randomized to the control group or treatment groups. Tumor volume and body weight were measured twice a week. Tumor volume was calculated as described previously [16]. T-DM1 was administered intravenously once every 3 weeks. As a control, saline was administered.

Flow cytometry analysis

Cells were labeled using trastuzumab or control HuIgG as the primary antibody followed by fluorescent labeling using PE mouse anti-human IgG antibody (BD Biosciences, San Jose, CA, USA) as the secondary antibody. Then the cell-surface HER2 expression was measured by flow cytometry. The cell-surface HER2 expression level was quantified as the mean fluorescence intensity (MFI) ratio, which was calculated as follows: MFI ratio = (MFI of sample labeled with trastuzumab)/(MFI of sample labeled with control HuIgG).

Western blotting

Cells were seeded onto six-well plates with $4–9 \times 10^5$ cells/well and were pre-cultured for 1 day or 2 days. To examine the HER2 expression level, cells were lysed in cell lysis buffer (Cell Signaling Technology, Danvers, MA, USA) containing protease inhibitor cocktail (Sigma-Aldrich) and phosphatase inhibitor cocktail (Nacalai Tesque, Kyoto, Japan). To examine HER2 signal inhibition and induction of apoptosis by T-DM1, the cells were first treated with T-DM1 for 24 h and then lysed as described above. Primary antibodies against HER2, HER3, phospho-HER3, EGFR, phospho-EGFR, Akt, phospho-Akt, ERK, phospho-ERK, β-actin (Cell Signaling Technology), cleaved PARP (Abcam, Cambridge, UK), and phospho-HER2 (Cell Signaling Technology and Abcam) were used. The detection was done by a capillary electrophoresis-based protein analysis system (Sally Sue; ProteinSimple, San Jose, CA, USA).

ADCC assay

KMCH-1 cells were collected, stained with calcein AM at 37 °C for 1 h, and plated on a U-bottomed 96-well plate at 2×10^4 cells/well. A dilution of each antibody (final concentrations: 10–0.000128 μg/mL) was added. CD16(158V)/NK-92 cells were used as the effector cell, and added to each well at an effector:target ratio of 4:1, 2:1, or 0:1. After 5 h incubation, supernatant was collected, and fluorescence intensity of calcein was measured using excitation at 490 nm and emission at 515 nm with a Varioskan LUX Multimode Microplate Reader (Thermo Fisher Scientific). %ADCC was calculated as follows: (sample release − low control)/(maximum release − low control) × 100. Low control means untreated KMCH-1 cells and maximum release means KMCH-1 cells lysed with 1% Triton X-100.

Cell cycle assay

Cells were seeded in 25 cm^2 flasks at 5×10^5 cells/flask and were pre-cultured for 1 day. The cells were then treated with 10 µg/mL of T-DM1, trastuzumab, or HuIgG for 24 h. Cells were collected and assayed with a BD Cycletest Plus DNA Kit (BD Biosciences). Cell cycle was analyzed with a flow cytometer.

Caspase 3/7 activity assay

Cells were seeded onto a 96-well plate at 1×10^4 cells/well and were pre-cultured for 1 day. The cells were then treated with 10 µg/mL of T-DM1, trastuzumab, or HuIgG for 24 h. Cells were assayed with the Caspase-Glo 3/7 Assay system (Promega, Fitchburg, WI, USA). Caspase 3/7 activity was measured with the POLARstar Omega microplate reader.

Immunohistochemistry (IHC) and fluorescence in situ hybridization (FISH)

IHC and FISH were, respectively, performed using HercepTest (Dako, Glostrup, Denmark) and PathVysion HER2 DNA Probe (Abbott Molecular, Abbott Park, IL, USA), as previously described [18]. HER2 gene copy number and HER2-to-CEP17 ratio were calculated by the FISH in accordance with PathVysion HER-2 DNA Probe Kit package insert. HER2 scoring was determined by SRL Medisearch (Tokyo, Japan) in accordance with the guidelines for breast cancer [19].

Statistical analysis

Statistical analysis was performed with JMP 11.2.1 (SAS Institute Japan, Tokyo, Japan).

Results

IHC staining and scoring of HER2 protein in gallbladder carcinoma and cholangiocarcinoma

Although many reports have shown the prevalence of HER2-positive BTC, their diagnostic methods sometimes lacked coherence. Therefore, we first performed IHC staining of HER2 protein using tissue microarrays derived from gallbladder carcinoma patients and cholangiocarcinoma patients and judged the HER2 status according to the method and criteria used for HER2 testing in breast cancer, in which T-DM1 has been used as a 2nd-line standard therapy. In the 80 cases present in the gallbladder carcinoma tissue microarray, 8 cases showed HER2 staining on the plasma membrane of tumor cells. Completely circumferential and strong membrane staining was observed in > 10% of tumor cells in 2 cases of adenocarcinoma (Fig. 1a, b) and 1 case of adenosquamous carcinoma (Fig. 1c), which were thus assessed as HER2 IHC score 3 +. Partially incomplete circumferential but moderate to strong staining was observed in > 10% of tumor cells in 1 case of adenocarcinoma (Fig. 1d) and 1 case of adenosquamous carcinoma (Fig. 1e), which were thus assessed as HER2 IHC score 2 +. Incompletely circumferential and weak to moderate membrane staining was observed in > 10% of tumor cells in 3 cases of adenocarcinoma (Fig. 1f–h), which were thus assessed as HER2 IHC score 1 +.

Of the cholangiocarcinoma specimens (54 cases), 2 showed HER2 staining. Although the staining was partial and weak, membrane staining of HER2 in > 10% of tumor cells was observed in both differentiated and undifferentiated types of cholangiocarcinoma (they were thus assessed as HER2 IHC score 1 +) (Fig. 1i, j).

In both the gallbladder carcinoma and the cholangiocarcinoma specimens that had differentiated ductal structures, HER2 staining was localized to the basolateral and lateral membranes of the tumors, and staining of the apical membrane was weak and only rarely observed, like it is in gastric cancer (Fig. 1a, b, d, f, g, i). However, our results suggested that both gallbladder carcinoma and cholangiocarcinoma express HER2, and that—in contrast to gastric cancer—little difference was observed between the differentiation stages [20, 21].

HER2 expression level and HER2 downstream signaling in the 17 BTC cell lines

IHC staining of HER2 in patients' gallbladder carcinoma and cholangiocarcinoma specimens indicated that T-DM1 could possibly show antitumor efficacy in BTC regardless of the degree of tumor differentiation. Thus, we investigated the efficacy of T-DM1 in BTC using several cell lines categorized as various pathological types. Because the antitumor activity of T-DM1 in several types of cancer, including breast cancer, depends mainly on the expression of HER2 and in part on its signaling, we first determined the cell-surface HER2 expression levels in BTC cell lines by flow cytometry and determined HER2 signal activation in the BTC cell lines by Western blot analysis. The seventeen BTC cell lines, comprising 6 cholangiocarcinoma cell lines, 7 gallbladder carcinoma cell lines, and 4 ampulla of Vater cell lines, were compared with 3 HER2-positive breast cancer cell lines: KPL-4 with a HER2 status score of 3 +|7.0[IHC score|HER2-to-CEP17 ratio by FISH testing], SK-BR-3 with a score 3 +|4.9, and MDA-MB-361with a score of 2 +|9.0 [22–24], or with a HER2-negative breast cancer cell line (MCF7 with a score of 0|1.3 [23]). HER2 expression higher than that in MCF7 was observed in KMCH-1,

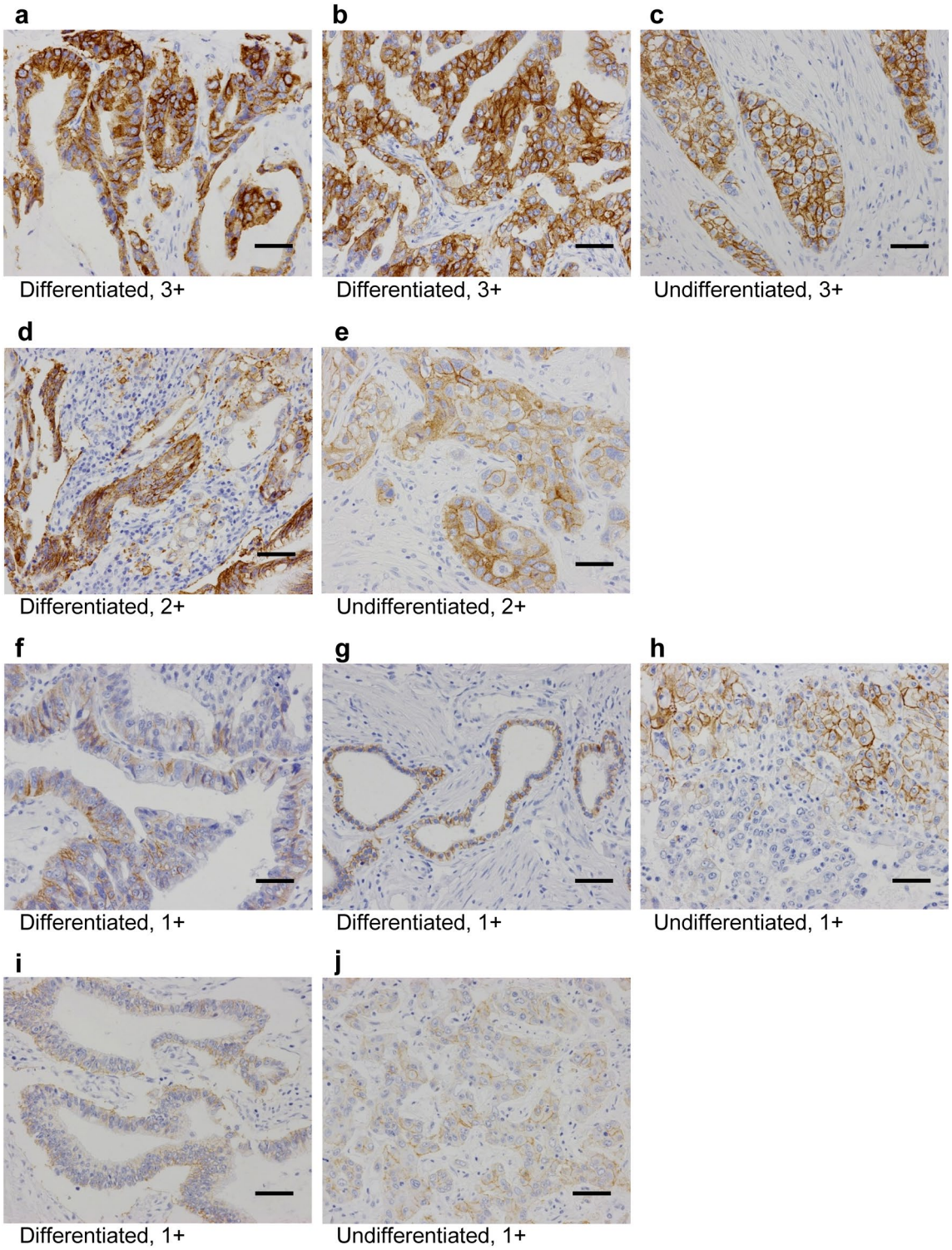

Fig. 1 HER2 expression in gallbladder carcinoma and cholangiocarcinoma. Tissue microarrays derived from patients with gallbladder carcinoma (**a–h**) and cholangiocarcinoma (**i, j**) were stained with HER2, and the IHC score was assessed. Scale bar 50 µm

Mz-ChA-1, and TGBC-18-TKB both by flow cytometry (Fig. 2a) and by Western blotting (Fig. 2b), and the other 14 BTC cell lines showed HER2 expression comparable to MCF7 (Fig. 2a). In parallel with these results for cell-surface HER2 expression, KMCH-1 and Mz-ChA-1 also showed clear phosphorylation of HER2 and HER3, similar

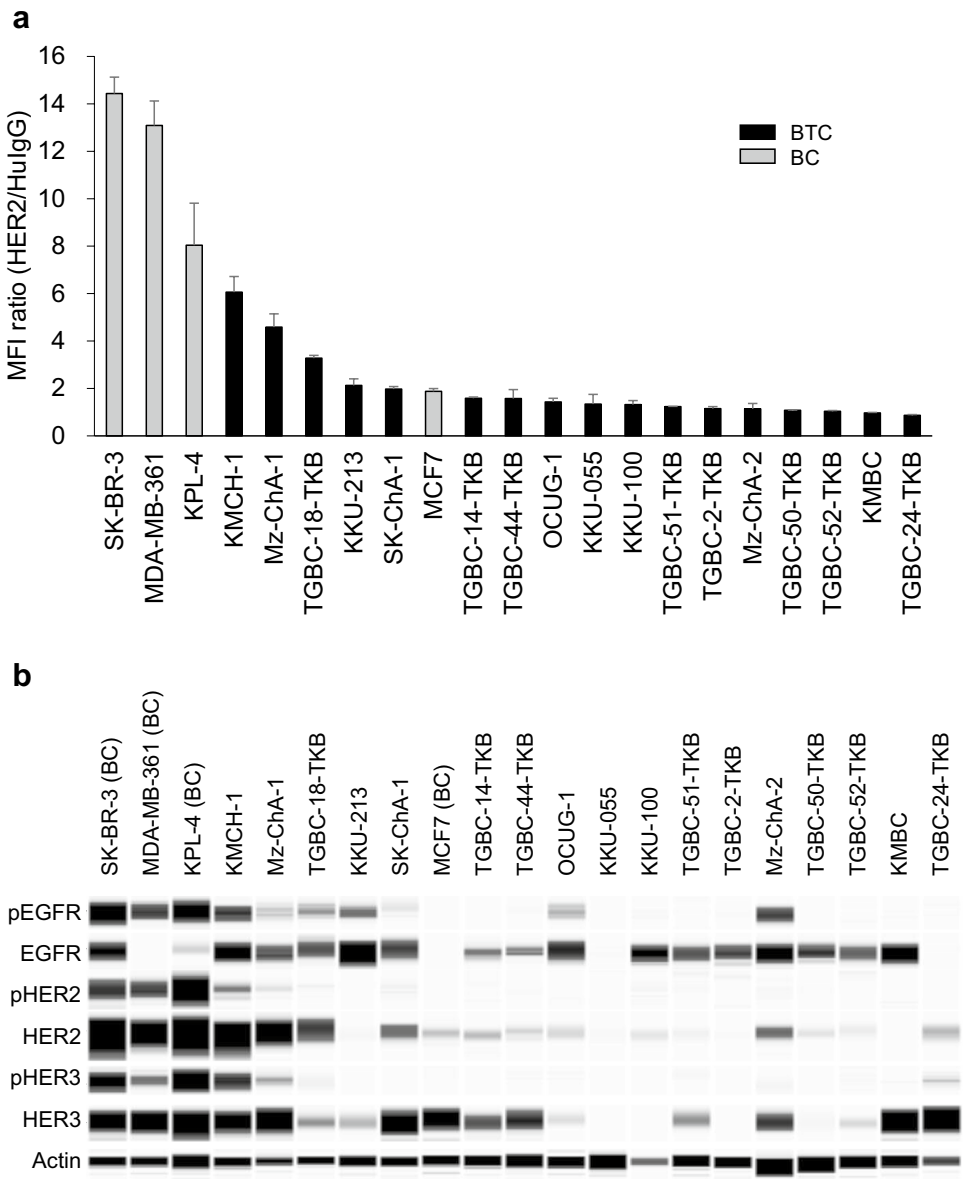

Fig. 2 HER2 expression and HER2-related signaling in BTC cell lines. **a** HER2 expression in 17 BTC and 4 breast cancer (BC) cell lines was detected by flow cytometry. **b** Total and phosphorylated EGFR, HER2, HER3, and their downstream molecules were detected by Western blotting. $n = 3$, mean + SD

to the levels seen in the 3 HER2-positive breast cancer cell lines (Fig. 2b).

Sensitivity of BTC cell lines to DM-1, gemcitabine, and T-DM1

To examine whether the sensitivity of BTC to T-DM1 is associated with the level of HER2 expression, its in vitro growth inhibition activity was tested. KMCH-1 was about ten times less sensitive to T-DM1 than the breast cancer cell lines SK-BR-3, MDA-MB-361, and KPL-4, which all showed higher HER2 expression (shown by the MFI ratio), but KMCH-1 was roughly as sensitive as MDA-MB-453. The sensitivity of Mz-ChA-1 and TGBC-18-TKB was comparable to that of ZR-75-1, and all three cell lines had an equivalent level of HER2 expression (Supplementary Table S1). The correlation of cell growth inhibition activity of T-DM1 in BTC cell lines with the cell-surface HER2 expression levels ($R^2 = 0.6127$) can also be seen in Fig. 3a, which shows that the correlation coefficient of BTC cell lines was not significantly different from that of breast cancer cell lines ($R^2 = 0.7622$, $P = 0.4884$). The cell growth inhibition activity of DM1 and gemcitabine, which is a chemotherapeutic agent used for BTC in general, did not correlate with the HER2 expression level ($R^2 = 0.1367$ and 0.0031, respectively) (Fig. 3b, c). Although the number of HER2-positive BTC cell lines was limited, the results show that in vitro anti-proliferative activity of T-DM1 in BTC would depend on HER2 expression.

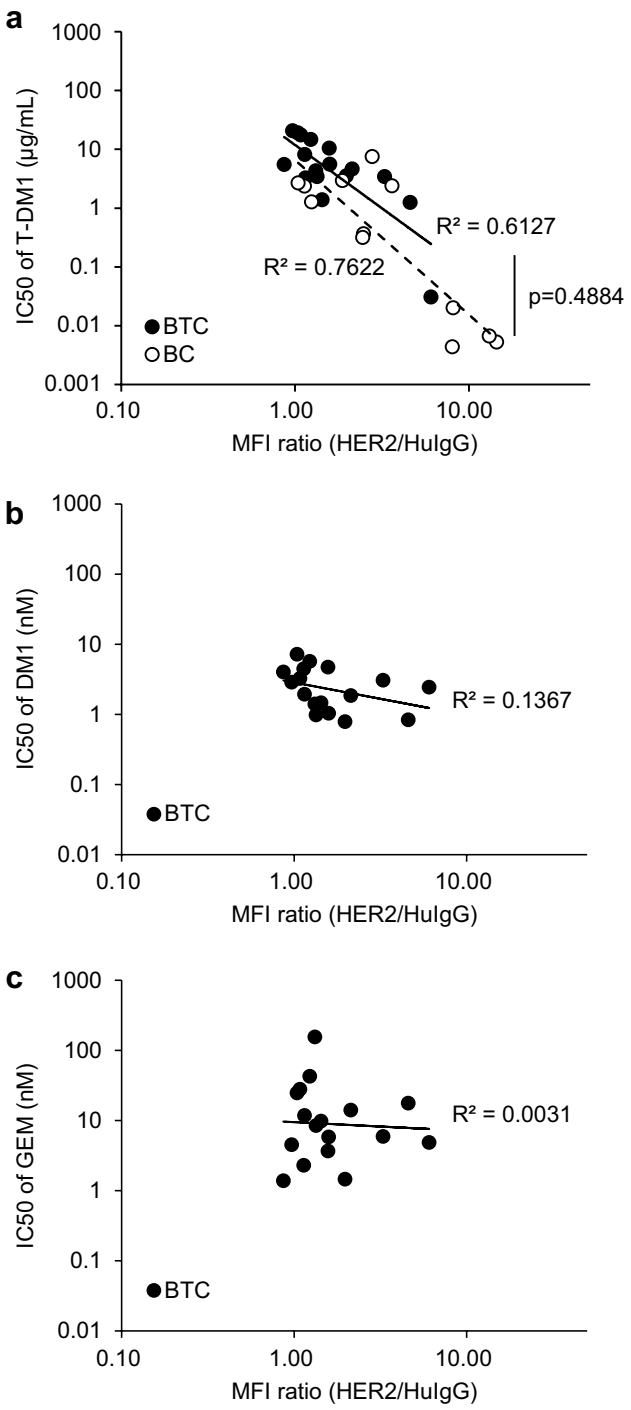

Fig. 3 Correlation between T-DM1, DM1, or gemcitabine efficacy and HER2 expression level in BTC cell lines. Cell growth inhibition by T-DM1, DM1, and gemcitabine (GEM) was detected and IC_{50} values were calculated in 17 BTC and 12 breast cancer cell lines. HER2 expression level was calculated from MFI by flow cytometry as the MFI ratio of HER2 to HuIgG. Correlation between HER2 expression levels and IC_{50} values of **a** T-DM1, **b** DM1, and **c** GEM were assessed in BTC cell lines. For T-DM1, the correlation was also compared with breast cancer cell lines. Statistical analysis was performed with the ANCOVA test

IHC and FISH assessment of HER2 in BTC xenografted tumors

To assess whether the antitumor efficacy of T-DM1 is dependent on HER2 level not only under cell culture conditions but also in mice, we established xenograft mouse models with BTC cells, with each model expressing a different level of HER2. We were successful in establishing 4 BTC xenograft models by implanting nude mice with the KMCH-1, Mz-ChA-1, OCUG-1, and KKU-100 cell lines.

Tumor specimens of KMCH-1 showed complete/intense circumferential membrane staining in > 10% of tumor cells; Mz-ChA-1 showed incomplete or weak/moderate circumferential membrane staining in > 10% of tumor cells; OCUG-1 showed incomplete, faint/barely perceptible membrane staining in > 10% of tumor cells, and KKU-100 showed no HER2 staining (Fig. 4a). According to the criteria used for assessing breast cancer, for which T-DM1 is approved [19], the HER2 IHC scores of the KMCH-1, Mz-ChA-1, OCUG-1, and KKU-100 models were assessed, respectively, as 3 + (HER2-positive), 2 + (HER2-equivocal), 1 +/0 (HER2-negative), and 0 (HER2-negative) (Table 1). Similarly, the HER2 FISH status (HER2-to-CEP17 ratio and gene copy number) of these models was, respectively, assessed as 8.3 and 20.1; 4.7 and 12.8; 1.4 and 4.2; and 1.1 and 2.6 (Table 1). These results determined the HER2 status of KMCH-1, Mz-ChA-1, OCUG-1, and KKU-100 models to be HER2-positive, HER2-positive, HER2-negative, and HER2-negative, respectively. Of these, the two HER2-positive models, KMCH-1 and Mz-ChA-1, were undifferentiated and differentiated type, respectively (Fig. 4a).

Antitumor activity of T-DM1 in BTC xenograft models

The antitumor activity of T-DM1 treatment given once every 3 weeks (q3w) was examined in the four BTC xenograft models. Significant antitumor efficacy at the indicated time points (see caption to Fig. 4) was observed for KMCH-1 and Mz-ChA-1 at all 3 dosages (5, 10, and 20 mg/kg), and for one dosage of OCUG-1 (20 mg/kg) (Fig. 4b). Tumor regression was observed in all mice ($n = 6$) treated with 20 mg/kg of T-DM1 in the KMCH-1 model. No significant antitumor efficacy was observed in the KKU-100 model, in which HER2 expression was not detected. These results suggest that T-DM1 exerts an in vivo antitumor efficacy in proportion to the level of HER2 expression on BTC cells.

Using the KMCH-1 xenograft model, we examined different dosing regimens to see which of them maximized the antitumor efficacy of T-DM1. Because the maximum tolerable dose of T-DM1 in humans in once-weekly dosing (qw) is two-thirds of that in q3w dosing (2.4 mg/kg and 3.6 mg/kg, respectively) [25] and because several

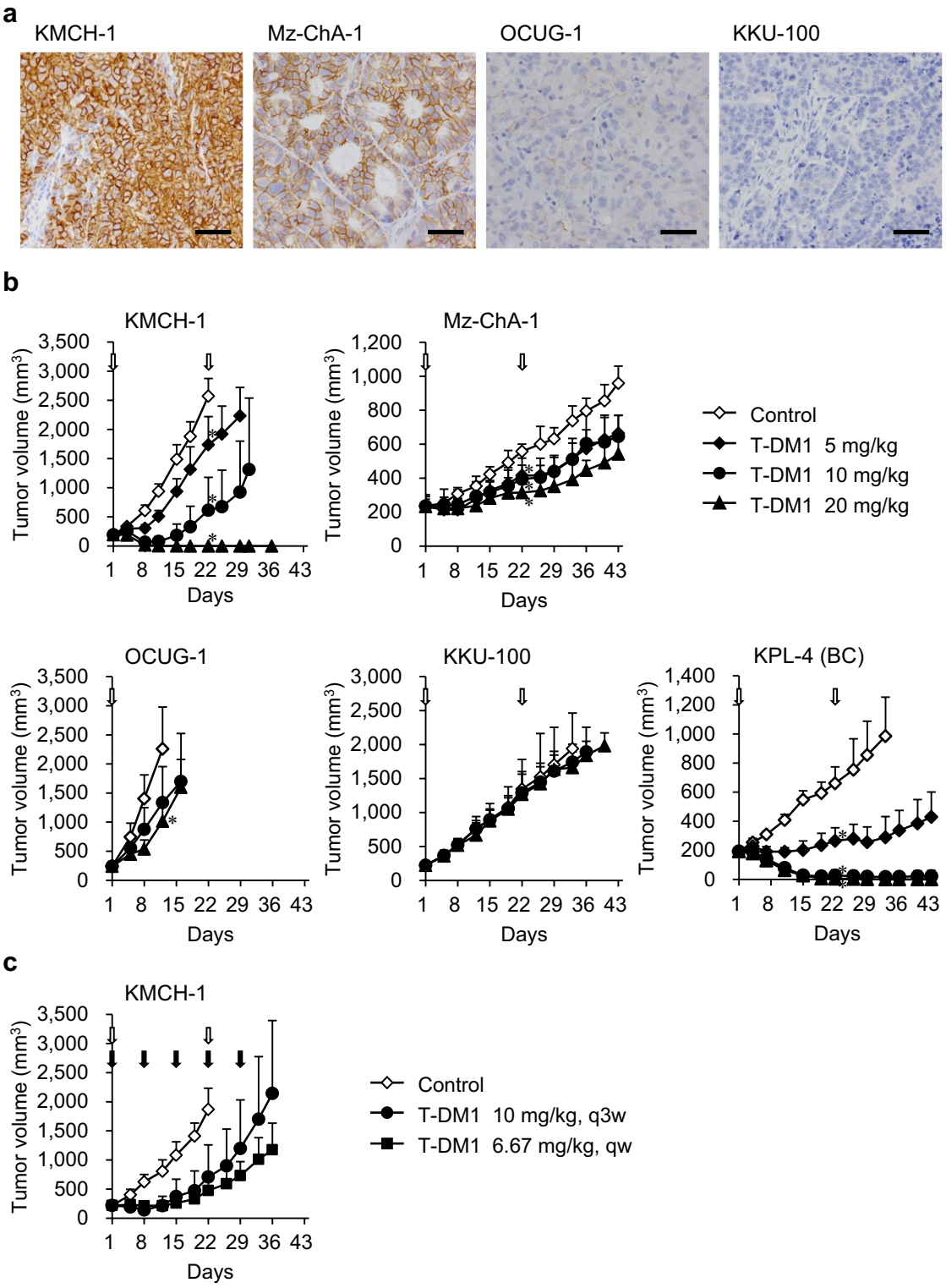

clinical studies have compared the efficacy and safety of 3.6 mg/kg of q3w and 2.4 mg/kg of qw administrations, this study compared the antitumor efficacy of 10 mg/kg of T-DM1 q3w and 6.67 mg/kg of T-DM1 qw. We found no significant difference in the antitumor efficacy between the two dosing groups (Fig. 4c). Our result suggests that more frequent administration of T-DM1 would not provide a large advantage in the treatment of BTC.

◂**Fig. 4** In vivo antitumor activity of T-DM1 in BTC cell line xenograft models. **a** HER2 expression and localization in tumor tissues from KMCH-1, Mz-ChA-1, OCUG-1, and KKU-100 xenograft models were assessed by IHC. Scale bar: 50 µm. **b** Antitumor activity of T-DM1 (5, 10, and 20 mg/kg) in xenograft models of KMCH-1, Mz-ChA-1, and KPL-4 (a breast cancer cell line), and that of T-DM1 (10 and 20 mg/kg) in OCUG-1 and KKU-100 xenograft models was assessed by measuring tumor volume twice a week. T-DM1 was intravenously administered on Days 1 and 22 (once every 3 weeks, shown by white arrows). As a control, saline was administered. **c** Antitumor activity of 10 mg/kg of T-DM1 administered on Days 1 and 22 (once every 3 weeks, shown by white arrows) compared with that of 6.67 mg/kg of T-DM1 administered on Days 1, 8, 15, 22, and 29 (once a week, shown by black arrows). Tumor volume was calculated twice a week. As a control, saline was administered. Statistical analysis was performed on Day 22, which was the last day of the first cycle of T-DM1 administration, in all except the OCUG-1 model. In the OCUG-1 model, statistical analysis was performed on Day 12 because the control group was abandoned on Day 12 due to tumor enlargement beyond the prescribed limit. $*P < 0.05$ by Steel's multiple comparison test vs. control group. Mean + SD, $n = 6$/group except for the study of OCUG-1 model ($n = 5$/group)

Table 1 HER2 status of tumor tissues used in biliary tract cancer xenograft models

	KMCH-1	Mz-ChA-1	OCUG-1	KKU-100
IHC score	3 +	2 +	1 +/0	0
FISH				
HER2-to-CEP17 ratio	8.3	4.7	1.4	1.1
Gene copy number	20.1	12.8	4.2	2.6
HER2 status	Positive	Positive	Negative	Negative

The mechanisms of action of T-DM1 in the BTC cell lines

To confirm whether the mode of action of T-DM1 is the same for BTC cells as it is for breast cancer cells, we examined the HER2 signal inhibition, ADCC, G2/M phase cell cycle arrest, and apoptosis that have been reported to be mediated by T-DM1 in breast cancer cells [13, 15, 26].

T-DM1 treatment of KMCH-1 cells reduced the phosphorylation levels of HER3 and downstream AKT and ERK, indicating that T-DM1 inhibited the formation of HER2–HER3 dimers (Fig. 5a). T-DM1 induced ADCC against KMCH-1 indicating an immune cell-mediated function of T-DM1 (Fig. 5b). T-DM1 caused cell cycle arrest in the G2/M phase, which indicates that DM1 is released intracellularly after internalization with HER2, as reported for other antibody–maytansinoid conjugates [27] (Fig. 5c). T-DM1 also increased sub-G0/G1 cells (Fig. 5c), and increased caspase 3/7 activity (Fig. 5d) and cleaved PARP expression (Fig. 5e), indicating that apoptosis was induced in KMCH-1 cells. These results suggested that all of the modes of action of T-DM1 reported for breast cancer cells are also seen in BTC cells.

Discussion

Gene amplification or protein overexpression of HER2 is a potent driver for cell proliferation, and these abnormal alterations are observed in many types of cancer including BTC. For HER2-overexpressing cancers, several anti-HER2 drugs including T-DM1 have been developed and these have improved the therapeutic outcomes of breast or gastric cancers. In this paper, we hypothesized that T-DM1 is a potential treatment for HER2-positive BTC, and we demonstrated two results, namely that the efficacy of T-DM1 in BTC cell lines depends on the level of HER2 expression and that sensitive cancers could be discerned by the same criteria as are used for breast cancer.

Because all activities of T-DM1—such as ADCC, inhibition of microtubule polymerization, and HER2 signal suppression—are produced through binding to cell-surface HER2 molecules, we screened 17 BTC cell lines by flow cytometry and Western blotting to determine their levels of HER2 expression. Although most cell lines expressed lower levels of HER2, we identified several cell lines with higher levels of HER2 expression. In addition, higher HER2-expressing BTC cell lines such as KMCH-1 showed both HER2 and HER3 phosphorylation, which indicated that HER2–HER3 heterodimers might play a potent role in HER2-overexpressing BTCs, as they do in breast cancers [28]. To construct xenograft models with which to evaluate T-DM1 efficacy, we tested the transplantability of these cell lines into nude mice, and assessed the HER2 expression levels of the xenografted tumors using the same diagnostic methods and criteria used clinically to assess breast cancer. Finally, we succeeded in establishing a xenograft panel for T-DM1 with four different HER2 IHC scores ranging from 0 to 3 +.

In these BTC models, the antitumor activity elicited by T-DM1 treatment was in proportion to their HER2 scores (Fig. 4). The efficacy of T-DM1 has also been reported to be dependent on HER2 expression in several other cancers. For breast cancer, T-DM1 showed higher antitumor efficacy towards cancers with higher HER2 gene expression in the TDM4258g trial (2nd line, phase II) [29]. In preclinical gastric cancer models, the antitumor effects of T-DM1 were in proportion to the HER2 status of the cancer [30, 31]. The efficacy of T-DM1 has also been demonstrated to be dependent on HER2 expression in non-small cell lung cancer cell lines [32] and bladder cancer cell lines [33]. It makes sense that the antitumor efficacy of T-DM1 in BTC is also dependent on HER2 expression or amplification. Of the BTC and breast cancer cell lines that overexpress HER2 in the current

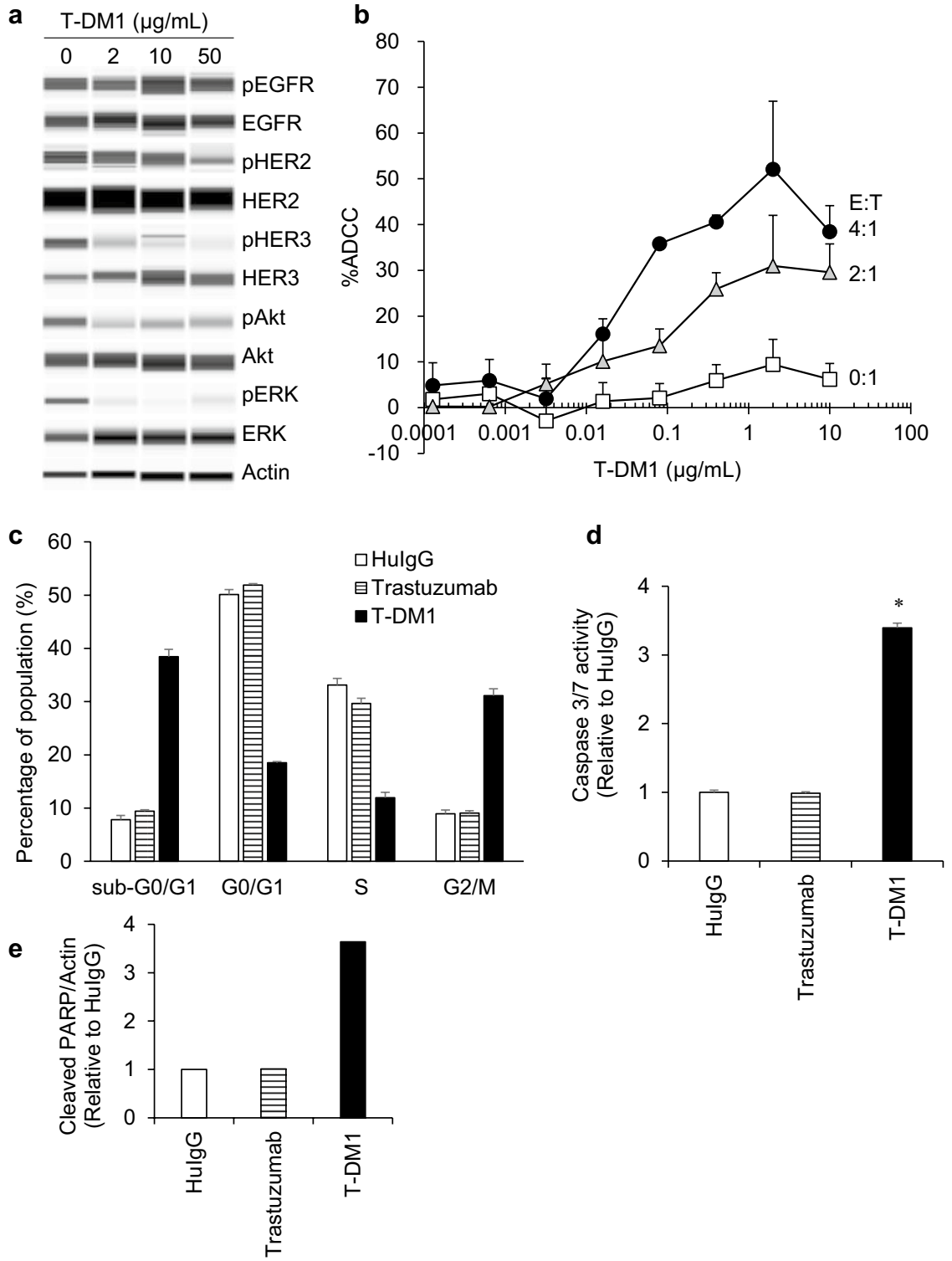

Fig. 5 Mechanism of action of T-DM1 in a BTC cell line. **a** Phosphorylation levels of HER2, EGFR, HER3, AKT, and ERK in the KMCH-1 cell line after 24 h of T-DM1 treatment, detected by Western blotting. **b** ADCC of T-DM1 in the KMCH-1 cell line was measured with calcein AM. E: effector cell. T: target cell. **c** Cell cycle analysis performed in KMCH-1 after 24 h of T-DM1 or trastuzumab treatment. Apoptosis induction was examined by **d** caspase 3/7 activity and **e** cleaved PARP expression in KMCH-1 after 24 h of T-DM1 or trastuzumab treatment. As a control, human IgG (HuIgG) was used. White bars, HuIgG-treated groups; banded bars, trastuzumab-treated groups; black bars, T-DM1-treated groups. $n = 3$ per group (**b, c**) and 5 per group (**d**), $^*P < 0.05$ by Dunnett's multiple comparison test vs. HuIgG group

study, the BTC cell line KMCH-1 showed lower sensitivity to T-DM1 in the cell growth inhibition assay and the mouse antitumor efficacy study than did the breast cancer cell lines SK-BR-3, MDA-MB-361, and KPL-4 (Supplementary Table S1, Fig. 4). However, we could not conclude that the sensitivity of BTC to T-DM1 was lower than that of breast cancer, considering that only one cell line, KMCH-1, was identified as HER2 IHC 3 + in the BTC cell lines we examined. Further preclinical and clinical studies are needed to clarify the T-DM1 sensitivity against BTC.

Our results showed some possible mechanisms by which T-DM1 acts on BTC cells. First, similar to its action in breast cancers, the DM1 released by intracellular digestion of T-DM1 inhibited tubulin polymerization and induced G2/M phase cell cycle arrest and apoptosis (Fig. 5c–e). Second, as reported in breast cancer cells, T-DM1 inhibited HER2 signaling that likely contributed to the suppression of cell growth (Fig. 5a). Third, as is also the case in breast cancer cells, T-DM1 activated ADCC (Fig. 5b), which would contribute to its antitumor efficacy in xenograft models. These results indicate that the modes of action of T-DM1 in BTC are equivalent to those in breast cancer.

When selecting cancers for which T-DM1 treatment will likely be effective, in addition to analyzing HER2 expression levels, histological analysis may also be helpful. In our current study, we employed the FISH- and ICH-scoring criteria used to analyze HER2 in breast cancer. However, the criteria used for histological assessment of HER2 status differ somewhat by type of cancer. For example, HER2 staining of gastric cancer is reported to differ from that of breast cancer in several ways: it is non-circumferential, localized to the basolateral membrane [34, 35]; it is stronger in well-differentiated intestinal-type cells than in undifferentiated diffuse-type cells [36]; and it exhibits intratumoral heterogeneity [37]. Although tissue microarray specimens from BTC showed U-shaped staining localized to the basolateral or lateral membranes in differentiated types (Fig. 1), there was no difference in the intensity of HER2 staining between differentiated and diffuse types in gallbladder carcinoma or cholangiocarcinoma. Thus, although the HER2 testing methods presently used would be valuable for discerning the BTC patients to whom T-DM1 therapy would be applicable, the histological properties of HER2 staining in BTC are not simply identical to those of breast cancer or of gastric cancer, and further basic and clinical research is necessary to identify the appropriate diagnostic criteria for assessing HER2 status in BTC patients.

In summary, we showed that the antitumor effect of T-DM1 in BTC is associated with HER2 expression level or gene amplification, the mode of action of T-DM1 in BTC is comparable to that in breast cancer, and that the methods presently used for HER2 testing can be applicable to BTC diagnosis, if the appropriate diagnostic criteria to select patients are ascertained. We hope that these findings will contribute to the evaluation of T-DM1 as a potential treatment for BTC.

Acknowledgements We thank Marie Mochizuki and Mirei Kouno (Product Research Department, Chugai Pharmaceutical Co., Ltd.) for technical assistance; Dr. Kaori Fujimoto-Ouchi (Product Research Department, Chugai Pharmaceutical Co., Ltd.) for helpful suggestions and comments about this study; and Dr. Banchob Spira (Khon Kaen University) for kindly providing KKU-100, KKU-055 and KKU-0213 cell lines.

Compliance with ethical standards

Conflict of interest Junichi Shoda received research fee and grants from Chugai Pharmaceutical Co., Ltd. and other authors have no conflict of interest.

Ethical standards All procedures performed in studies involving human participants were in accordance with the ethical standards of the institutional research committee at Chugai Pharmaceuticals, Co., Ltd. and with the 1964 Helsinki declaration and its later amendments or comparable ethical standards. The human tissues were processed anonymously inhibiting the revelation of the donor's identity.

References

1. Chan E, Berlin J (2015) Biliary tract cancers: understudied and poorly understood. J Clin Oncol 33(16):1845–1848. https://doi.org/10.1200/jco.2014.59.7591
2. Recio-Boiles A, Babiker HM (2017) Cancer, gallbladder. In: StatPearls. StatPearls, Treasure Island
3. Furuse J, Okusaka T (2011) Targeted therapy for biliary tract cancer. Cancers (Basel) 3(2):2243
4. Yarden Y, Sliwkowski MX (2001) Untangling the ErbB signalling network. Nat Rev Mol Cell Biol 2:127. https://doi.org/10.1038/35052073
5. Wang Z (2017) ErbB receptors and cancer. In: Wang Z (ed) ErbB receptor signaling: methods and protocols. Springer, New York, pp 3–35. https://doi.org/10.1007/978-1-4939-7219-7_1
6. Chua TC, Merrett ND (2012) Clinicopathologic factors associated with HER2-positive gastric cancer and its impact on survival outcomes—a systematic review. Int J Cancer 130(12):2845–2856. https://doi.org/10.1002/ijc.26292
7. Wong H, Yau T (2012) Targeted therapy in the management of advanced gastric cancer: are we making progress in the era of personalized medicine? Oncologist 17(3):346–358. https://doi.org/10.1634/theoncologist.2011-0311
8. Terashima M, Kitada K, Ochiai A, Ichikawa W, Kurahashi I, Sakuramoto S, Katai H, Sano T, Imamura H, Sasako M, Group A-G (2012) Impact of expression of human epidermal growth factor receptors EGFR and ERBB2 on survival in stage II/III gastric cancer. Clin Cancer Res 18(21):5992–6000. https://doi.org/10.1158/1078-0432.CCR-12-1318
9. Galdy S, Lamarca A, McNamara MG, Hubner RA, Cella CA, Fazio N, Valle JW (2017) HER2/HER3 pathway in biliary tract malignancies; systematic review and meta-analysis: a potential therapeutic target? Cancer Metastasis Rev 36(1):141–157. https://doi.org/10.1007/s10555-016-9645-x
10. Nam AR, Kim JW, Cha Y, Ha H, Park JE, Bang JH, Jin MH, Lee KH, Kim TY, Han SW, Im SA, Kim TY, Oh DY, Bang YJ (2016) Therapeutic implication of HER2 in advanced biliary tract cancer.

Oncotarget 7(36):58007–58021. https://doi.org/10.18632/oncotarget.11157
11. Kawamoto T, Ishige K, Thomas M, Yamashita-Kashima Y, Shu S, Ishikura N, Ariizumi S, Yamamoto M, Kurosaki K, Shoda J (2015) Overexpression and gene amplification of EGFR, HER2, and HER3 in biliary tract carcinomas, and the possibility for therapy with the HER2-targeting antibody pertuzumab. J Gastroenterol 50(4):467–479. https://doi.org/10.1007/s00535-014-0984-5
12. Erickson HK, Park PU, Widdison WC, Kovtun YV, Garrett LM, Hoffman K, Lutz RJ, Goldmacher VS, Blattler WA (2006) Antibody-maytansinoid conjugates are activated in targeted cancer cells by lysosomal degradation and linker-dependent intracellular processing. Cancer Res 66(8):4426–4433. https://doi.org/10.1158/0008-5472.can-05-4489
13. Barok M, Tanner M, Koninki K, Isola J (2011) Trastuzumab-DM1 causes tumour growth inhibition by mitotic catastrophe in trastuzumab-resistant breast cancer cells in vivo. Breast Cancer Res 13(2):R46. https://doi.org/10.1186/bcr2868
14. Oroudjev E, Lopus M, Wilson L, Audette C, Provenzano C, Erickson H, Kovtun Y, Chari R, Jordan MA (2010) Maytansinoid-antibody conjugates induce mitotic arrest by suppressing microtubule dynamic instability. Mol Cancer Ther 9(10):2700–2713. https://doi.org/10.1158/1535-7163.mct-10-0645
15. Junttila TT, Li G, Parsons K, Phillips GL, Sliwkowski MX (2011) Trastuzumab-DM1 (T-DM1) retains all the mechanisms of action of trastuzumab and efficiently inhibits growth of lapatinib insensitive breast cancer. Breast Cancer Res Treat 128(2):347–356. https://doi.org/10.1007/s10549-010-1090-x
16. Yamashita-Kashima Y, Shu S, Yorozu K, Moriya Y, Harada N (2017) Mode of action of pertuzumab in combination with trastuzumab plus docetaxel therapy in a HER2-positive breast cancer xenograft model. Oncol Lett 14(4):4197–4205. https://doi.org/10.3892/ol.2017.6679
17. Yamashita-Kashima Y, Iijima S, Yorozu K, Furugaki K, Kurasawa M, Ohta M, Fujimoto-Ouchi K (2011) Pertuzumab in combination with trastuzumab shows significantly enhanced antitumor activity in HER2-positive human gastric cancer xenograft models. Clin Cancer Res 17(15):5060–5070. https://doi.org/10.1158/1078-0432.CCR-10-2927
18. Yamashita-Kashima Y, Shu S, Yorozu K, Hashizume K, Moriya Y, Fujimoto-Ouchi K, Harada N (2014) Importance of formalin fixing conditions for HER2 testing in gastric cancer: immunohistochemical staining and fluorescence in situ hybridization. Gastric Cancer 17(4):638–647. https://doi.org/10.1007/s10120-013-0329-8
19. Wolff AC, Hammond MEH, Hicks DG, Dowsett M, McShane LM, Allison KH, Allred DC, Bartlett JMS, Bilous M, Fitzgibbons P, Hanna W, Jenkins RB, Mangu PB, Paik S, Perez EA, Press MF, Spears PA, Vance GH, Viale G, Hayes DF (2013) Recommendations for Human Epidermal Growth Factor Receptor 2 testing in breast cancer: American Society of Clinical Oncology/College of American Pathologists Clinical Practice Guideline Update. J Clin Oncol 31(31):3997–4013. https://doi.org/10.1200/JCO.2013.50.9984
20. Stephen L, Bastiaan DBW, Soraya F, Michael P, Priyanthi KM (2011) Human epidermal growth factor receptor 2 testing in gastric carcinoma: issues related to heterogeneity in biopsies and resections*. Histopathology 59(5):832–840. https://doi.org/10.1111/j.1365-2559.2011.04017.x
21. Tanner M, Hollmén M, Junttila TT, Kapanen AI, Tommola S, Soini Y, Helin H, Salo J, Joensuu H, Sihvo E, Elenius K, Isola J (2005) Amplification of HER-2 in gastric carcinoma: association with Topoisomerase IIα gene amplification, intestinal type, poor prognosis and sensitivity to trastuzumab. Ann Oncol 16(2):273–278. https://doi.org/10.1093/annonc/mdi064
22. Fujimoto-Ouchi K, Sekiguchi F, Yasuno H, Moriya Y, Mori K, Tanaka Y (2007) Antitumor activity of trastuzumab in combination with chemotherapy in human gastric cancer xenograft models. Cancer Chemother Pharmacol 59(6):795–805. https://doi.org/10.1007/s00280-006-0337-z
23. Li Y, Zhang R, Han Y, Lu T, Ding J, Zhang K, Lin G, Xie J, Li J (2016) Comparison of the types of candidate reference samples for quality control of human epidermal growth factor receptor 2 status detection. Diagn Pathol 11(1):85. https://doi.org/10.1186/s13000-016-0537-8
24. Kim SY, Kim HP, Kim YJ, Oh DY, Im SA, Lee D, Jong HS, Kim TY, Bang YJ (2008) Trastuzumab inhibits the growth of human gastric cancer cell lines with HER2 amplification synergistically with cisplatin. Int J Oncol 32(1):89–95. https://doi.org/10.3892/ijo.32.1.89
25. Beeram M, Krop IE, Burris HA, Girish SR, Yu W, Lu MW, Holden SN, Modi S (2012) A phase 1 study of weekly dosing of trastuzumab emtansine (T-DM1) in patients with advanced human epidermal growth factor 2-positive breast cancer. Cancer 118(23):5733–5740. https://doi.org/10.1002/cncr.27622
26. Lewis Phillips GD, Li G, Dugger DL, Crocker LM, Parsons KL, Mai E, Blattler WA, Lambert JM, Chari RV, Lutz RJ, Wong WL, Jacobson FS, Koeppen H, Schwall RH, Kenkare-Mitra SR, Spencer SD, Sliwkowski MX (2008) Targeting HER2-positive breast cancer with trastuzumab-DM1, an antibody-cytotoxic drug conjugate. Cancer Res 68(22):9280–9290. https://doi.org/10.1158/0008-5472.can-08-1776
27. Erickson HK, Park PU, Widdison WC, Kovtun YV, Garrett LM, Hoffman K, Lutz RJ, Goldmacher VS, Blättler WA (2006) Antibody-maytansinoid conjugates are activated in targeted cancer cells by lysosomal degradation and linker-dependent intracellular processing. Cancer Res 66(8):4426–4433. https://doi.org/10.1158/0008-5472.can-05-4489
28. Baselga J, Swain SM (2009) Novel anticancer targets: revisiting ERBB2 and discovering ERBB3. Nat Rev Cancer 9(7):463–475. https://doi.org/10.1038/nrc2656
29. Burris HA 3rd, Rugo HS, Vukelja SJ, Vogel CL, Borson RA, Limentani S, Tan-Chiu E, Krop IE, Michaelson RA, Girish S, Amler L, Zheng M, Chu YW, Klencke B, O'Shaughnessy JA (2011) Phase II study of the antibody drug conjugate trastuzumab-DM1 for the treatment of human epidermal growth factor receptor 2 (HER2)-positive breast cancer after prior HER2-directed therapy. J Clin Oncol 29(4):398–405. https://doi.org/10.1200/jco.2010.29.5865
30. Barok M, Tanner M, Koninki K, Isola J (2011) Trastuzumab-DM1 is highly effective in preclinical models of HER2-positive gastric cancer. Cancer Lett 306(2):171–179. https://doi.org/10.1016/j.canlet.2011.03.002
31. Yamashita-Kashima Y, Shu S, Harada N, Fujimoto-Ouchi K (2013) Enhanced antitumor activity of trastuzumab emtansine (T-DM1) in combination with pertuzumab in a HER2-positive gastric cancer model. Oncol Rep 30(3):1087–1093. https://doi.org/10.3892/or.2013.2547
32. Cretella D, Saccani F, Quaini F, Frati C, Lagrasta C, Bonelli M, Caffarra C, Cavazzoni A, Fumarola C, Galetti M, La Monica S, Ampollini L, Tiseo M, Ardizzoni A, Petronini PG, Alfieri RR (2014) Trastuzumab emtansine is active on HER-2 overexpressing NSCLC cell lines and overcomes gefitinib resistance. Mol Cancer 13:143. https://doi.org/10.1186/1476-4598-13-143
33. Hayashi T, Seiler R, Oo HZ, Jager W, Moskalev I, Awrey S, Dejima T, Todenhofer T, Li N, Fazli L, Matsubara A, Black PC (2015) Targeting HER2 with T-DM1, an antibody cytotoxic drug conjugate, is Effective in HER2 over expressing bladder cancer. J Urol 194(4):1120–1131. https://doi.org/10.1016/j.juro.2015.05.087

34. Hofmann M, Stoss O, Shi D, Buttner R, van de Vijver M, Kim W, Ochiai A, Ruschoff J, Henkel T (2008) Assessment of a HER2 scoring system for gastric cancer: results from a validation study. Histopathology 52(7):797–805. https://doi.org/10.1111/j.1365-2559.2008.03028.x
35. Bang YJ, Van Cutsem E, Feyereislova A, Chung HC, Shen L, Sawaki A, Lordick F, Ohtsu A, Omuro Y, Satoh T, Aprile G, Kulikov E, Hill J, Lehle M, Ruschoff J, Kang YK (2010) Trastuzumab in combination with chemotherapy versus chemotherapy alone for treatment of HER2-positive advanced gastric or gastro-oesophageal junction cancer (ToGA): a phase 3, open-label, randomised controlled trial. Lancet 376(9742):687–697. https://doi.org/10.1016/s0140-6736(10)61121-x
36. Van Cutsem E, Bang Y-J, Feng-yi F, Xu JM, Lee K-W, Jiao S-C, Chong JL, López-Sanchez RI, Price T, Gladkov O, Stoss O, Hill J, Ng V, Lehle M, Thomas M, Kiermaier A, Rüschoff J (2015) HER2 screening data from ToGA: targeting HER2 in gastric and gastroesophageal junction cancer. Gastric Cancer 18(3):476–484. https://doi.org/10.1007/s10120-014-0402-y
37. Lee HE, Park KU, Yoo SB, Nam SK, Park DJ, Kim HH, Lee HS (2013) Clinical significance of intratumoral HER2 heterogeneity in gastric cancer. Eur J Cancer 49(6):1448–1457. https://doi.org/10.1016/j.ejca.2012.10.018

Affiliations

Yoriko Yamashita-Kashima[1] · Yasushi Yoshimura[1] · Takaaki Fujimura[1] · Sei Shu[1] · Mieko Yanagisawa[1] · Keigo Yorozu[1] · Koh Furugaki[1] · Ryota Higuchi[2] · Junichi Shoda[3] · Naoki Harada[1]

[1] Product Research Department, Chugai Pharmaceutical Co., Ltd., 200 Kajiwara, Kamakura, Kanagawa 247-8530, Japan

[2] Department of Gastroenterological Surgery, Tokyo Women's Medical University, 8-1 Kawada-cho, Shinjuku-ku, Tokyo 162-8666, Japan

[3] Department of Medical Sciences, Faculty of Medicine, University of Tsukuba, 1-1-1 Tennodai, Tsukuba, Ibaraki 305-8575, Japan